Volume 34, issue 2, April 2013    ISSN NO 0141-9382

# Displays

Contains Special Issue Articles – The Applied Issues in Visual
Perception and Action

Guest Editors: Richard H.Y. So and Li Li

**Displays**

# Saccade detection during smooth tracking

Dorion B. Liston [a,b,*], Anton E. Krukowski [a,b], Leland S. Stone [a]

[a] *NASA Ames Research Center, Moffett Field, California 94035, United States*
[b] *San José State University, San José, California 95192, United States*

ABSTRACT

Saccade detection in an eye-movement trace provides a starting point for analyses ranging from the investigation of low-level oculomotor mechanisms to high-level cognitive processes. When the eye tracks the motion of the object of current interest (smooth pursuit), of the visual background (OKN), or of the resultant visual motion from a head movement (tVOR, rVOR), the smooth tracking movement is generally intermixed with rapid-phase saccadic eye movements, which must be excised to analyze the smooth components of tracking behavior properly. We describe a simple method to detect saccades on a background trace of variable velocity, compare our saccade-detection algorithm with the performance of an expert human observer, and present an ideal-observer analysis to benchmark its detection performance.

© 2012 Elsevier B.V. All rights reserved.

## 1. Introduction

Saccade detection in an eye-movement trace provides a starting point for analyses ranging from the investigation of low-level oculomotor mechanisms to high-level cognitive processes. For example, metrics provided by the saccadic main sequence [1,2] allow for quantitative diagnosis of saccadic abnormalities [3]; intra-saccadic intervals define fixation duration, dwell time, and scanpath information useful to address perceptual or cognitive processing [4–7]; the proportion or frequency of saccades during smooth movement can be used as metrics to assess VOR failure [8], smooth pursuit pathology [9,10], or to evaluate display motion quality [11,12]. Filters for saccade detection have been developed and refined over several decades [13–16], often adjusted according to the experimental question and the eye-tracker signal quality at hand. In this paper, we propose a novel method designed to detect saccades superimposed on smooth tracking recorded using non-invasive video-based eye trackers (typically with position noise levels of more than a tenth of a degree). Previous methods using velocity and/or acceleration thresholds [15,17] work quite well with invasive eye tracking systems (e.g., eye coils) with eye-position noise on the order of a hundredth of a degree, but cannot be used robustly with video-based tracker data.

The smooth eye-movement responses to the motion of the object of current interest (smooth pursuit), of the visual background (OKN), or of the observer's head (tVOR, rVOR) is generally intermixed with rapid phase saccadic eye movements. To extract the information about cognitive, perceptual, and oculomotor function associated with saccades, a robust signal-processing method is needed to detect saccadic "pulses" superimposed on a background of varying "smooth" velocity [18], especially when the background velocity distorts the familiar saccadic velocity profile (e.g., catch-back saccades). Furthermore, correctly de-saccaded traces are an assumed starting point for any number of analyses of smooth movements: analysis of smooth tracking [19–21], perception–action linkages [22], assessment of visual stability during optokinetic nystagmus [23,24], or VOR compensation for translational [25–27] and rotational [8,28–30] head movements. To this end, we describe a simple method to detect saccades on a background trace of variable velocity, present an ideal-observer analysis to benchmark its detection performance, and compare our saccade-detection algorithm with the performance of an expert human observer on simulated trials with realistic background velocity profiles.
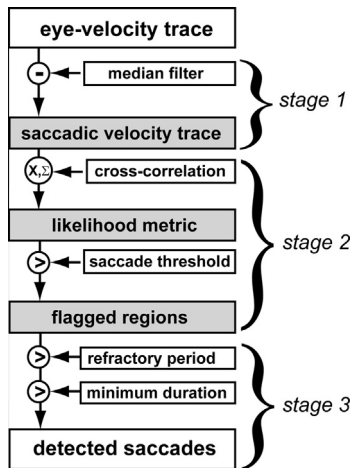
## 2. Algorithm

Our saccade-detection algorithm has three stages starting from the original eye-velocity trace (Fig. 1). The first stage uses a median filter to process the eye-velocity trace in such a way as to cancel out the velocity components related to smooth tracking. The second stage is a linear detector based on an ideal observer approach [31] that measures saccade likelihood at every sample during the movement, and uses a threshold parameter to flag potential saccade regions. The third stage is a clustering stage [32] to mitigate the effects of temporal uncertainty and tracker noise, and to reduce false alarms from noise transients.

### 2.1. Stage 1 – non-linear median filtering

Given a velocity trace at a known sampling rate, the first step is to estimate the smooth component of the oculomotor response

* Corresponding author at: NASA Ames Research Center, Mail Stop 262-2, Moffett Field, CA 94035, United States. Tel.: +1 650 604 4065; fax: +1 650 604 0255.
*E-mail address:* dorion.b.liston@nasa.gov (D.B. Liston).

**Fig. 1.** Algorithmic steps. The first stage in the algorithm is to calculate the median filter, which is then subtracted from the original velocity trace to yield a saccadic velocity trace. The second stage takes the cross-correlation between the saccadic velocity trace and a saccade velocity template, yielding a likelihood metric. As the cross-correlation involves integration over time, the units of the likelihood metric are expressed in degrees rather than degrees per second; regions of the trace that exceed the threshold. The third stage compares the flagged regions against a minimum inter-saccadic refractory period and a minimum saccadic duration, combining nearby flagged regions and turning off regions less than a minimum duration. Regions that conform to these criteria are then detected as saccadic movements.

using a "median filter". The median-filtered trace is computed by sliding a window of odd size over the velocity trace, replacing each sample of the original trace with the median velocity inside the window [33], the size of which is one parameter of our algorithm. The output of this filter is then subtracted from the original veloc-

ity trace [34] yielding a "saccadic velocity" trace. Given a well-chosen window size, the median filter behaves similar to a low-pass filtered version of the original trace [8] except that the high-frequency saccadic velocity components remain largely intact, an interesting and critical nonlinear advantage of the median.

### 2.2. Stage 2 – linear template matching

We then take the cross-correlation between the eye-velocity trace and a saccadic velocity template as in similar approaches [13], which yields a likelihood metric [31] for saccade occurrence. The saccade-velocity template [35]

$$Velocity\_template(t) = \frac{35 \cdot amp}{16 \cdot duration} \left( 1 - \frac{4t^2}{duration^2} \right)^3 \tag{1}$$

is scaled such that the value of the likelihood metric approximately equals the estimated saccade amplitude.

$$scale\_factor = \frac{\int velocity\_template}{sampling\_frequency \cdot \int velocity\_template^2} \tag{2}$$

Because the cross-correlation involves integration (i.e., the dot product of the saccade template and a template-sized window around each sample in the velocity trace), the units of the likelihood metric are expressed in degrees rather than degrees per second. Portions of the eye-movement trace where the likelihood metric exceeds the threshold are then flagged using the threshold parameter, specified in degrees.

### 2.3. Stage 3 – non-linear clustering

Brief flagged regions occurring in rapid succession less than a minimum refractory period apart are combined into a unified sac-
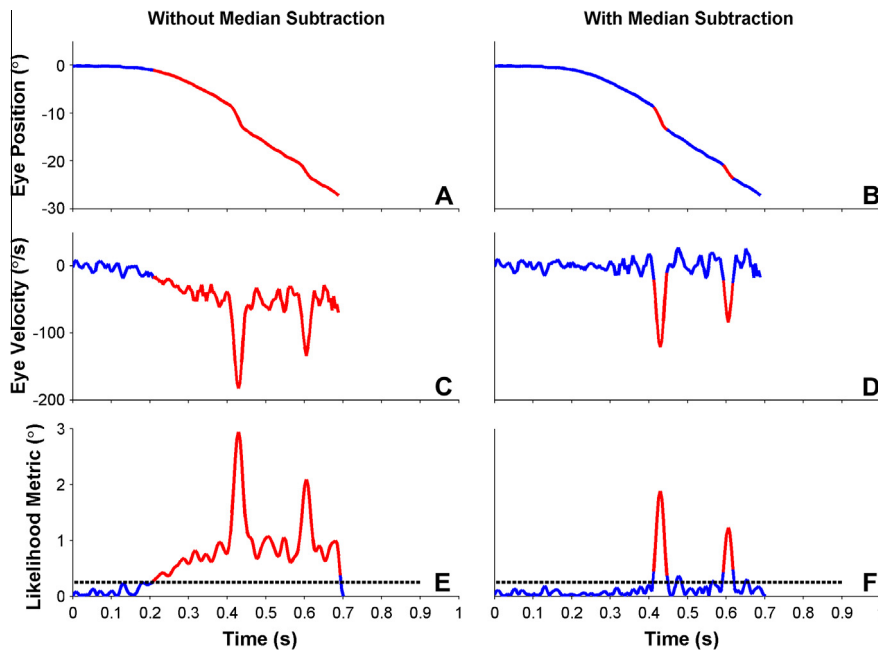


**Fig. 2.** Effect of median filter on detection of saccades during tracking. A–B plot one horizontal eye-position response to a 80 deg/s moving target spot containing pursuit and saccades detected (solid red) without (A) and with (B) median subtraction, sampled at 240 Hz with a video-based ISCAN tracker. Velocity traces are generated by applying a FIR low-pass differentiating filter (−3 DB at 32 Hz) to eye position. These filtered velocity traces are an attempt to isolate the velocities associated with saccadic movements, which is done much more successfully with the median filter (D) than without (C), illustrating the difference between the "saccadic velocity trace" (D) and the velocity trace containing both smooth and saccadic components (C). E–F plot our saccade likelihood metric showing how simple thresholding can cleanly detect saccades in the median filter case. The median filter allows the resolution of the three separate saccades along with minimization of any false positive portions of the trace (caused by tracker and biological noise). For this example, the width of the median filter was set to 170 ms (41 samples), the threshold (dashed black line) was set to 0.25° and the minimum saccade duration was 16 ms. On standard desktop hardware (3.2 GHz CPU), the Matlab implementation of this detection algorithm requires 226 ms of computation time for this ~2 s trial (1.3 s fixation period not shown).

cade, preventing the measurement of partial saccades and avoiding misses. Flagged regions greater than a minimum saccade duration are simply retained as saccades for further processing; isolated brief flagged periods are de-flagged as presumed false alarms. This additional processing involves two floating parameters: the minimum saccade duration and the minimum refractory period (shortest time between two saccades). Given the noise level in eye position and using the saccadic main sequence, a useful criterion for the minimum saccade duration is the expected saccadic duration for a movement "in the noise", with amplitude equal to eye position noise (i.e., a noise level of 0.15° corresponds roughly to a duration of 10 ms from Eq. (1)) [36]. A useful minimum refractory period under common circumstances (16 ms, four samples at 240 Hz) would consider "saccades" separated by only one, two, or three samples (12 ms) as a single unified saccade with the missed thresholding arising from noise in the eye position trace during the saccade. Saccade detection in tasks that elicit rapid back-to-back saccades or movements that turn around in mid-flight [37] may require reducing the minimum refractory period.

## 3. Results

The median filtering allows us to estimate the smooth component of the tracking response to be removed from the velocity trace [34], leaving the high-frequency saccadic components largely intact (Fig. 2). To preserve these components, the size of the median filter must be at least twice the width of the largest saccade to be detected, and need not be fine-tuned as a function of smooth velocity (a window size of 100–200 ms provides robust results for velocities up to 60 deg/s).

### 3.1. Comparison with human expert detection

The threshold parameter in our algorithm determines the trade-off between hits and false alarms (Fig. 3), akin to setting the criterion in a decision problem [31]. To explore this tradeoff in determining the best-choice value of the threshold parameter for real data, we compare the empirical distribution of saccadic amplitudes hand-identified by an expert human observer analyzing real human tracking trials (Fig. 2, blue distributions) with the distribution of saccade amplitudes detected by our algorithm in simulated trials (solid black). The threshold parameter of our algorithm varied from 0.20° to 0.60°. In the test data set, observers were asked to track a small laser spot moving at speeds ranging from 10 deg/s to 25 deg/s. Eye-position signals were recorded using an ISCAN video-based eye-tracking system (RK-726 PCI), with a noise level of ∼0.10° [38]. If the threshold parameter is too low, the detector starts to return small false alarm saccades (see red portion of the plot near zero for a threshold of 0.20°); if the threshold parameter is too high, small saccades will be missed. Assuming that the true distribution of saccade amplitudes is unimodal, even expert human observers have a small apparent tendency to identify noise as sacc-
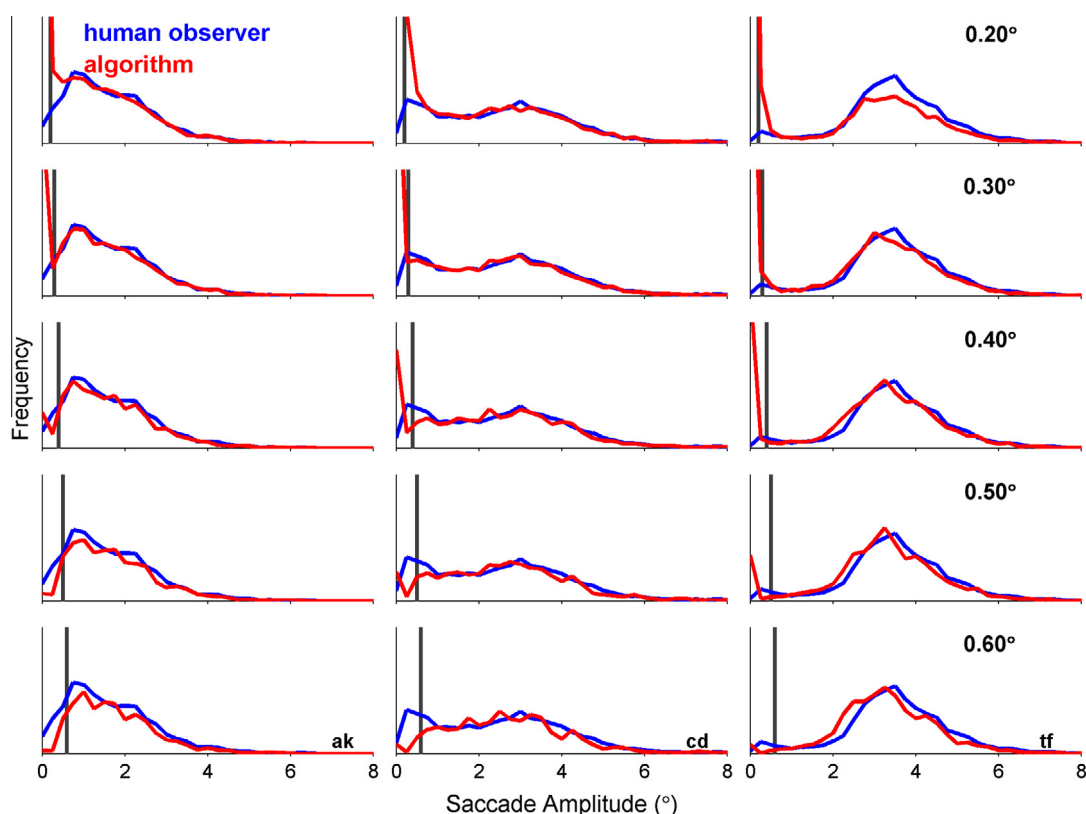


**Fig. 3.** Performance of detection algorithm versus expert human observer. The distributions of hand-cut saccades (blue distributions) are shown for three observers (columns) on a smooth-pursuit task [38], in comparison with distribution of amplitudes using our saccade-detection algorithm (red distributions). For each observer, we simulated the original set of trials (800 trials, 800 ms in duration, $\sigma_{tracker}$ = 0.1°) using the list of observed saccade amplitudes and their temporal occurrences. We then used our algorithm to flag saccades and estimate their amplitudes. Each column represents data from one observer; each row shows the distribution of flagged amplitudes at a given threshold. Other detection parameters are similar to those used in the original analysis (median window: 170 ms, minimum duration: 12 ms). Vertical gray lines show the threshold level used in that simulation. When the threshold was set too low (0.20°), the algorithm returned false alarms by flagging noise as small movements (peaks in red distribution near zero). When the threshold was set too high (0.60°), the algorithm missed some saccades. For these data, a threshold of ∼0.30–0.40° best approximates the shape of the original hand-measured distribution, albeit with an obvious peak for very small false alarm saccades. This peak could be eliminated by re-using the amplitude parameter to screen all saccades smaller than the threshold, at the cost of missing real saccades of this amplitude.
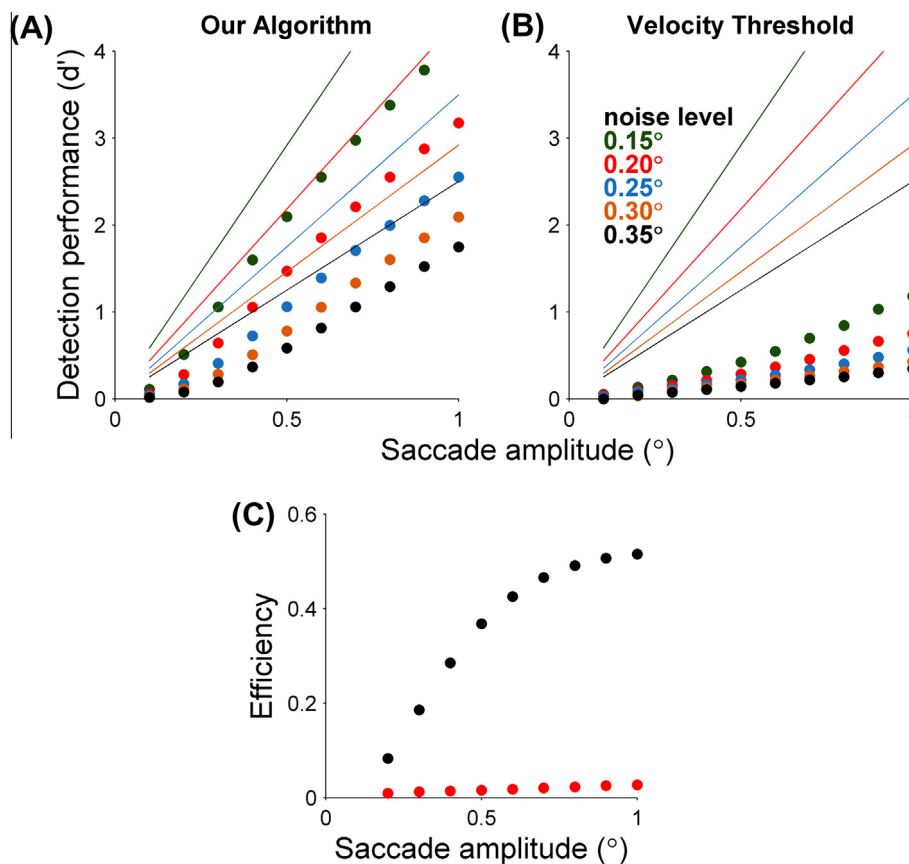
**Fig. 4.** Performance comparison of algorithm and standard velocity threshold. Solid lines in A–B plot detection performance ($d'$ for the YES–NO detection task) for the ideal observer as a function of saccade amplitude in the signal-known-exactly case. Colors represent increasing levels of eye-position noise, ranging from 0.15° (green) to 0.35° (black). Filled circles plot detection performance for the current algorithm (A) and a standard velocity threshold (B). Panel C plots the efficiency ($d'/d'_{ideal}$)$^2$ for the current algorithm (black filled circles) and the velocity threshold (red filled circles) detector as a function of saccade amplitude, averaged across the five noise levels. This simulation tested the effect of noise level on detection performance for a very brief (28 ms) velocity trace, the threshold for both detectors was allowed to vary with the simulated saccade amplitude (current algorithm: amplitude/2; velocity threshold: peak_velocity /*.75). The median filter and minimum refractory period for the current algorithm were turned off in this simulation; minimum saccade duration was set to 16 ms.

adic movements (see small mode near zero for observers cd and tf). The false alarm performance of our automated algorithm is only slightly worse than a human expert for thresholds in the 0.30° range, indicating that that value approximates the threshold employed by expert human observers. Erring toward a low threshold (reduces missed saccades, increases false alarms) is generally less troublesome than a high threshold (some small saccades will be missed and thus included in any smooth movement analysis), as the minimum saccade duration effectively reduces false alarms.

### 3.2. Comparison with previous algorithms

An ideal observer provides a useful benchmark to evaluate the performance of our saccade detection algorithm under varying conditions, from the simplest ideal case to more realistic conditions. The task of the ideal observer in the signal-known-exactly condition is to report whether or not a saccade of known amplitude, direction, duration, and timing occurred, given a velocity trace. In this case, the ideal observer takes the cross-correlation between the known saccade velocity template and the corresponding samples in the velocity trace, and computes a single value which is then compared to a criterion to report whether or not a saccade occurred [31]. This cross-correlation approach defines the upper limit for detection performance ($d'$ in the YES–NO task, plotted as solid lines in Fig. 4A–B), against which we compared the performance of our algorithm (Fig. 4A) as well as another common approach,

a fixed velocity threshold (Fig. 4B) [39], for various levels of eye-tracker noise. Under realistic saccade-detection conditions, unknown saccade timing introduces temporal uncertainty into the trial, compromising the detection performance of our algorithm as well as the fixed-velocity threshold. In this simulation, we explore the effect varying levels of eye-position noise, which smoothly degrades detection performance of both algorithms, with efficiencies (($d'_{detector}$)$^2$/($d'_{ideal}$)$^2$) of less than 0.05 for a simple velocity threshold and up to 0.50 for our algorithm.

### 3.3. Setting the floating parameters

The median filter size should be set using the basic heuristic that it be at least twice the duration of the largest saccade expected in the data. In our analyses, we commonly used a median filter size of 164 ms. Saccade threshold should be set to detect saccades larger than the noise level in the eye-position trace, approximately 0.2–0.25° for eye-position noise of 0.15°. Minimum saccade duration should be set to the duration of a saccade "in the noise", approximately 16 ms; values either too high or too low will compromise saccade detection, as described below. The minimum refractory period should be at least 16 ms unless rapid back-to-back saccades are expected.

Saccade-detectors must detect saccades above an arbitrary size and operate over the entire trial, thus identifying any above-threshold values as saccades and returning a troublesome number
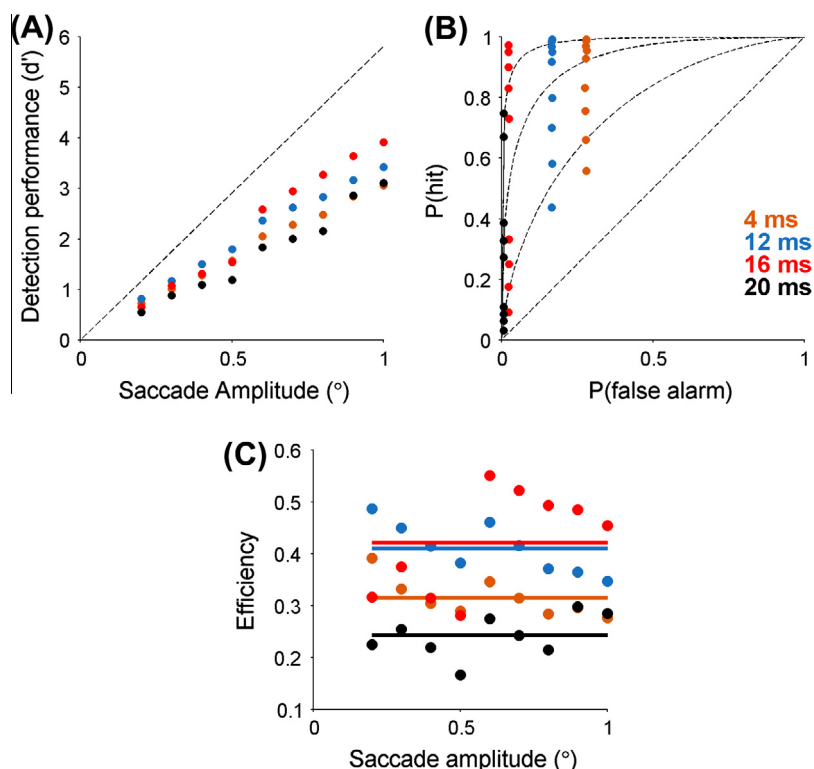
**Fig. 5.** Using the minimum saccade duration parameter to mitigate false alarms caused by temporal uncertainty. In A, the solid red line plots theoretical detection performance for the ideal observer (slope = 5.82 given $\sigma_{\text{tracker}} = 0.15°$, [22]) for a signal specified exactly (no uncertainty in amplitude, onset time, or duration). In the simulation of our linear detector phase, our algorithm performs a YES–NO task deciding whether a short velocity trace (28 ms in duration) contains a saccade of unknown amplitude, onset time, and duration. The cross-correlation metric uses a fixed saccade template (7 samples, 28 ms in length). Because onset time is not known, cross-correlation values are taken at each point in the velocity filter trace and all values of the correlation metric that exceed a fixed detection threshold (0.25°) are flagged as possible saccades, increasing both the hit and false alarm rates. The color series of filled circles illustrate the mitigating effect of minimum saccade duration on detection performance. Note that as minimum duration increases, efficiency increases until a maximum value of 16 ms (trf) at which point efficiency decreases again. B illustrates this further by plotting the proportion of hit responses (a "saccade present" response when a saccade is present) as a function of the proportion of false alarms (a "saccade present" response when no saccade is present). Dashed black lines represent $d'$ values of 0, 1, 2, and 3 in this YES–NO task. Each filled circle in C plots the efficiency of our algorithm as a function of saccade amplitude using a given value of minimum saccade duration (color series given in B). Dashed horizontal lines plot the average efficiency across all amplitudes tested. As the minimum duration increases up to 16 ms (blue) false alarms systematically decrease, but as it increases further to 20 ms (black), hits begin to decrease lowering efficiency as shown in C. The minimum duration should be set to a value less than half the duration of the smallest saccade of interest (i.e., 12–16 ms, 3–4 samples at 240 Hz).

of false alarms. Our minimum saccade duration parameter [40] preferentially decreases false alarms up to a point, but will diminish detection performance if set too high (Fig. 5A). We used our algorithm to detect generic saccades (unknown amplitude, onset time, and duration) within simulated trials that closely matched the ideal observer's task, using very short (28-ms) traces. Using a fixed detection threshold (0.25°), we plotted the effect of a minimum saccade duration parameter that ranged from no effective minimum (yellow) to 20 ms (black). As shown in this simulation, the minimum saccade duration parameter decreases the proportion of both hits and false alarms, which can both help and hinder detection performance depending on how well the minimum duration is tuned to saccade size.

The efficiency of our algorithm in detecting generic saccades (unknown amplitude, direction, duration, and timing) clearly varies as a function of minimum duration. The efficiency of our algorithm starts at ~30% with no minimum duration, increases to ~40% for a minimum of 12–16 ms, and then decreases again to 25% at 20 ms. In addition, the fixed 28-ms saccade template clearly helps detect saccades of amplitude 0.6° or greater, apparent in the clear discontinuity in performance at that amplitude. Further refinements to the algorithm could include: use of acceleration signals to detect saccade onsets and offsets [15], padding the flagged region on either side to account for the sub-threshold velocity wings of the saccade, throwing out saccades with amplitudes smaller than the saccade threshold, modification of acausal filters and implementation in a low-level language that will allow for near real-time saccade-detection during an experiment, and employing the main sequence relationships in a more sophisticated way to ensure that the peak velocity, duration, and amplitude are consistent with actual saccades.

## 4. Discussion

We describe a simple saccade-detection algorithm derived from an ideal-observer based approach, with several novel advantages. Using a well-tuned median filter, we effectively subtract out low-frequency components of the velocity trace related to smooth tracking while leaving saccadic components effectively unperturbed. Whereas any realistic linear high-pass filter will attenuate the high-frequency components of the saccade, median subtraction leaves them largely intact. Next, the cross-correlation between the velocity trace and a saccade-shaped velocity profile is generated and thresholded to identify portions of the trace corresponding to likely saccade occurrences. Detecting saccades using cross-correlation with a ~30 ms template attenuates high-frequency eye-tracker noise and allows the saccade threshold parameter to be expressed in position rather than velocity units, with detection performance that smoothly degrades as noise levels

increase. Finally, a minimum saccade duration is imposed to keep the false-alarm rate at an acceptable level. The four parameters of our algorithm (median-filter window size, saccade amplitude threshold, minimum saccade duration, minimum refractory period) allow straightforward comparison of the signal-to-noise properties of our algorithm with that of an ideal linear detector. In our simulations, our algorithm detects generic saccades (uncertainty in onset time, amplitude, and duration) with performance up to 0.50 of that of an ideal observer facing no temporal or amplitude uncertainty.

## Acknowledgements

## References

[1] D.A. Robinson, The mechanics of human saccadic eye movement, J. Physiol. 174 (1964) 245–264.

[2] A.T. Bahill, M.R. Clark, L. Stark, The main sequence, a tool for studying human eye movements, Math. Biosci. 24 (1975) 191–204.

[3] R.J. Leigh, D.S. Zee. The Neurology of Eye Movements, Oxford University Press, New York, NY, 2006.

[4] D. Noton, L. Stark, Scanpaths in eye movements during pattern perception, Science 171 (1971) 308–311.

[5] R.H.S. Carpenter, S.A. McDonald, LATER predicts saccade latency distributions in reading, Exp. Brain Res. 177 (2007) 176–183.

[6] R.P. Rao, G.J. Zelinsky, M.M. Hayhoe, D.H. Ballard, Eye movements in iconic visual search, Vision Res. 42 (2002) 1447–1463.

[7] K. Rayner, Eye guidance in reading: fixation locations within words, Perception 8 (1979) 21–30.

[8] R. Jell, G. Turnipseed, F. Guedry, Digital Analysis of the Voluntary Head Movement-Induced Vestibulo-Ocular Reflex With Saccade Extraction, NAMRL-1271, Naval Aerospace Medical Research Laboratory, Pensacola, FL, 1980.

[9] S. Levin, A. Luebke, D.S. Zee, T.C. Hain, D.A. Robinson, P.S. Holzman, Smooth pursuit eye movements in schizophrenics: quantitative measurements with the search-coil technique, J. Psychiatr. Res. 22 (1988) 195–206.

[10] G.U. Lekwuwa, G.R. Barnes, C.J. Collins, P. Limousin, Progressive bradykinesia and hypokinesia of ocular pursuit in Parkinson's disease, J. Neurol. Neurosurg. Psychiatry 66 (1999) 746–753.

[11] Y. Kuroki, T. Nishi, S. Kobayashi, H. Oyaizu, S. Yoshimura, Improvement of motion image quality by high frame rate, SID Symp. Dig. Tech. Papers 37 (2006) 14–17.

[12] B.T. Sweet, L.S. Stone, D.B. Liston, T.M. Herbert, Effects of spatio-temporal aliasing on out-the-window visual systems, IMAGE conference abstract; 2008.

[13] J.R. Tole, L.R. Young, Digital filters for saccade and fixation detection, in: D.F. Fisher, R.A. Monty, J.W. Senders (Eds.), Eye Movements: Cognition and Visual Perception, L. Erlbaum Associates, Hillsdale, NJ, 1981.

[14] D. Sauter, B.J. Martin, N. Di Renzo, C. Vomscheid, Analysis of eye tracking movements using innovations generated by a Kalman filter, Med. Biol. Eng. Comput. 29 (1991) 63–69.

[15] R.J. Krauzlis, F.A. Miles, Decreases in the latency of smooth pursuit and saccadic eye movements produced by the "gap paradigm" in the monkey, Vision Res. 36 (1996) 1973–1985.

[16] A. Duchowski, E. Medlin, N. Cournia, H. Murphy, A. Gramopadhye, S. Nair, J. Vorah, B. Melloy, 3-D eye movement analysis, Behav. Res. Methods Instrum. Comput. 34 (2002) 573–591.

[17] S.G. Lisberger, Postsaccadic enhancement of initiation of smooth pursuit eye movements in monkeys, J. Neurophysiol. 79 (1998) 1918–1930.

[18] G.R. Barnes, A procedure for the analysis of nystagmus and other eye movements, Aviat. Space Environ. Med. 53 (1982) 676–682.

[19] D.A. Robinson, The mechanics of human smooth pursuit eye movement, J. Physiol. 180 (1965) 569–591.

[20] M.M. Churchland, S.G. Lisberger, Experimental and computational analysis of monkey smooth pursuit eye movements, J. Neurophysiol. 86 (2001) 741–759.

[21] S.G. Lisberger, L.E. Westbrook, Properties of visual inputs that initiate horizontal smooth pursuit eye movements in monkeys, J. Neurosci. 5 (1985) 1662–1673.

[22] L.S. Stone, B.R. Beutter, J. Lorenceau, Visual motion integration for perception and pursuit, Perception 29 (2000) 771–787.

[23] A. Kaminiarz, B. Krekelberg, F. Bremmer, Localization of visual targets during optokinetic eye movements, Vision Res. 47 (2007) 869–878.

[24] A. Kaminiarz, B. Krekelberg, F. Bremmer, Expansion of visual space during optokinetic afternystagmus (OKAN), J. Neurophysiol. 99 (2008) 2470–2478.

[25] G.D. Paige, D.L. Tomko, Eye movement responses to linear head motion in the squirrel monkey. I. Basic characteristics, J. Neurophysiol. 65 (1991) 1170–1182.

[26] G.D. Paige, S.H. Seidman, Characteristics of the VOR in response to linear acceleration, Ann. NY Acad. Sci. 871 (1999) 123–135.

[27] M. Shelhamer, D.C. Roberts, D.S. Zee, Dynamics of the human linear vestibulo-ocular reflex at medium frequency and modification by short-term training, J. Vestib. Res. 10 (2000) 271–282.

[28] R. Ramachandran, S.G. Lisberger, Normal performance and expression of learning in the vestibulo-ocular reflex (VOR) at high frequencies, J. Neurophysiol. 93 (2005) 2028–2038.

[29] E.L. Keller, Gain of the vestibulo-ocular reflex in monkey at high rotational frequencies, Vision Res. 18 (1978) 311–315.

[30] U.W. Buettner, V. Henn, L.R. Young, Frequency response of the vestibulo-ocular reflex (VOR) in the monkey, Aviat. Space Environ. Med. 52 (1981) 73–77.

[31] D.M. Green, J.A. Swets, Signal Detection Theory and Psychophysics, Wiley, New York, 1966.

[32] M. Nystrom, K. Holmqvist, An adaptive algorithm for fixation, saccade, and glissade detection in eyetracking data, Behav. Res. Methods 42 (2010) 188–204.

[33] S.K. Mitra, Digital signal processing: a computer-based approach, 4th ed., McGraw-Hill, Boston, 2011.

[34] J.M. Leiser, System identification of horizontal oculomotor tracking, M.S. Thesis, Mechanical and Aeronautical Engineering, University of California, Davis, 2001.

[35] M.A. Garcia-Perez, E. Peli, Intrasaccadic perception, J. Neurosci. 21 (2001) 7313–7322.

[36] S. Martinez-Conde, S.L. Macknik, D.H. Hubel, The role of fixational eye movements in visual perception, Nat. Rev. Neurosci. 5 (2004) 229–240.

[37] D.B. Liston, L.S. Stone, Effects of prior information and reward on oculomotor and perceptual choices, J. Neurosci. 28 (2008) 13866–13875.

[38] A.E. Krukowski, L.S. Stone, Expansion of direction space around the cardinal axes revealed by smooth pursuit eye movements, Neuron 45 (2005) 315–323.

[39] D.D. Salvucci, J.H. Goldberg, Identifying fixations and saccades in eye-tracking protocols, in: Proceedings of the Eye Tracking Research & Applications, Symposium, 2000, pp. 71–78.

[40] M.R. Harwood, L.E. Mezey, C.M. Harris, The spectral main sequence of human saccades, J. Neurosci. 19 (1999) 9098–9106.